Electrician : Jurnal Rekayasa dan Teknologi Elektro
Vol. 20 No. 02, e-ISSN:2549-3442 http://dx.doi.org/10.23960/elc.v20.n2.2991

Hysteresis Direct Torque Control of Unity Voltage Ratio Indirect Matrix Converter for Variable-Speed Induction Motor Drive

Wahyu Cahyo Hidayat[1*], Charles Ronald Harahap[2], FX Arinto Setyawan[3]

[1,2,3] Jurusan Teknik Elektro Universitas Lampung; Jl. Prof. Soemantri Brojonegoro No. 1 Bandar Lampung 35145; Telp. +62721702673

Received: 03-11-2025
Accepted: 27-11-2025

Keywords:
Indirect Matrix Converter;
Direct Torque Control;
Variable Speed Drive;
Unity Voltage Transfer Ratio;
AC–AC Power Conversion.

Corespondent Email:
wahyucahyo.h@gmail.com

Abstract. *This paper evaluates the performance of a unity–voltage-transfer-ratio Indirect Matrix Converter (IMC) supplying a three-phase induction motor under hysteresis-based Direct Torque Control (DTC). The objective is to verify whether a unity-ratio IMC (previously validated only for passive loads) can operate reliably in variable-speed motor-drive applications. The main contribution is a comprehensive assessment of speed dynamics, torque-flux regulation, converter voltage behavior, and transient response when driving an 11-kW induction machine. A complete MATLAB/Simulink model is developed, incorporating an AC/AC boost stage, a current-source rectifier, a clamp and braking circuit, and a voltage-source inverter governed by hysteresis DTC with an outer-loop PI speed controller. The procedure involves no-load tests and step-load disturbances at multiple operating frequencies to evaluate steady-state performance and dynamic behavior. The results show that the IMC maintains a stable fictitious DC-link voltage, generates balanced output voltages, and achieves sinusoidal input currents with controllable power flow. The motor exhibits smooth acceleration, slip between 0 and 0.98%, and torque-recovery times of approximately 0.43-0.54 s after load perturbations. These findings demonstrate that the unity-ratio IMC is suitable for high-performance induction-motor drives and provide a foundation for future research on enhanced AC/AC converter topologies.*

1. INTRODUCTION

Advances in electrical energy conversion demand efficient and compact control systems for induction motors. Induction motors remain prevalent across industrial applications because of their inherently simple design, minimal servicing requirements, and high operational reliability. For optimal performance, they require precise speed control with variable voltage and frequency supply [1], [2], [3], [4]. Motor speed control is commonly achieved using AC–DC–AC inverter system (VSD); however, they suffer from drawbacks such as large DC-link capacitors, reduced reliability, and increased harmonic distortion that degrades power quality [5], [6].

Hironimus et al. (2024) reported that three- phase induction motors serve as the primary drives in industrial systems such as mining conveyors and are typically controlled by conventional AC–DC–AC variable speed drives. This indicates that improving motor drive quality, particularly through AC–AC conversion technologies such as the Indirect Matrix Converter, can potentially enhance efficiency and power quality in industrial applications [7]. Literature studies show that Venturini modulation is the fundamental technique in matrix converters, serving as an AC–AC converter without a DC link. With technological progress,matrix converters have evolved into Indirect Matrix Converters (IMC), Sparse IMC, and Ultra-Sparse IMC, along with advanced topologies such as Z-source, multilevel, and multiphase converters. Modern modulation strategies, including space vector modulation and indirect SVM, have been developed to improve voltage transfer ratio, efficiency, and system reliability. Therefore,

research on matrix converters continues actively, with Venturini modulation remaining the foundation for next-generation AC–AC converter innovations [8].

Mentari et al. demonstrated the capability of the Direct Matrix Converter (DMC) employing Venturini modulation to achieve speed regulation of a three-phase induction machine through both simulation and experimental validation. The system produced rotational performance consistent with induction motor theory and maintained good power quality at the fifth and seventh harmonics, although the third harmonic remained relatively high. Their later work further validated these findings by applying an Indirect Space Vector Modulation (ISVM) based matrix converter in a closed-loop system, achieving stable AC–AC frequency and amplitude control without a DC link using a PI controller [9].

Zaen et al. demonstrated that combining Space Vector Modulation (SVM) with Sliding Mode Control (SMC) enhances transient performance of induction motors by lowering overshoot to 0.50% and reducing settling time to 0.05 seconds, surpassing conventional matrix converters. These findings highlight Venturini-based DMC as the core foundation for modern modulation and control developments in induction motor drives [10]. Conversely, the Indirect Matrix Converter (IMC) has emerged as an advanced alternative that overcomes the inherent restriction of the DMC, particularly its peak voltage transfer capability limited to 0.866.

Jahangiri and Radan [11] proposed a modified IMC topology incorporating an AC/AC boost chopper to achieve a unity voltage transfer ratio without additional reactive elements or complex control techniques, while maintaining key advantages such as controllable input power factor, sinusoidal current, and bidirectional power flow. Simulation and prototype results showed strong voltage boosting while maintaining system integrity. Overall, prior studies highlight the progression of matrix converter technology from basic Venturini modulation toward the IMC as a more advanced AC–AC conversion approach.

This study is motivated by the main limitation of conventional matrix converters, namely the maximum voltage transfer ratio of 0.866, which prevents the output voltage from reaching the full input level [11], [12], [13], [14]. To overcome this limitation, the study employs an Indirect Matrix Converter (IMC) topology capable of achieving a unity voltage transfer ratio, as proposed by Jahangiri and Radan [11]. The previous study evaluated the IMC only under a static load composed of a 5 mH inductor and an 8 Ω resistor, without validating its use in a variable-speed three- phase induction motor drive. This leaves a gap in understanding how a unity-ratio IMC performs in VSD applications, particularly in motor speed dynamics, power-transfer efficiency, and output-voltage quality.

This study analyzes the performance of the Indirect Matrix Converter (IMC) with a unity voltage transfer ratio for driving a three-phase induction motor, using detailed modeling and simulation, and compares the results with established motor characteristics. The main contribution is a comprehensive assessment of the unity-ratio IMC in Variable Speed Drive applications, emphasizing dynamic response, power conversion efficiency, and output voltage quality, aspects that have not been quantitatively addressed in earlier studies.

2. LITERATURE REVIEW

2.1. Matrix Converter

A matrix converter is an AC–AC conversion topology that provides a direct linkage between a three-phase source and a three-phase load with fully controllable output frequency and amplitude, while eliminating the need for a DC-link rectification stage. By eliminating the need for DC-side capacitors, matrix converters offer boosted power density, a smaller form factor, and better reliability than classical AC–DC–AC converters.

A conventional matrix converter consists of nine bidirectional power switches arranged in a 3×3 switching structure, allowing any of the three output phases (A, B, and C) to be linked to any of the three input phases (a, b, and c), as shown in Figure 1 below. Beyond offering independent control of the output voltage magnitude and frequency, the MC supports reverse power transfer, generates nearly sinusoidal waveforms at both the input and output, and enables input power-factor regulation. These capabilities make it well suited for three-phase induction motor drives and modern industrial applications that demand high efficiency and performance [15].

Two primary configurations exist within the matrix-converter family, namely the Direct Matrix Converter (DMC) and the Indirect Matrix Converter (IMC). A DMC uses a 3×3 matrix of nine bidirectional switches for direct input–output connection, while an IMC relies on a virtual DC stage without capacitors, making it easier to implement and control. Other variants, including sparse and ultra sparse IMCs as well as Z-source and quasi Z-source matrix converters, have been introduced to improve voltage transfer capability and efficiency [16].

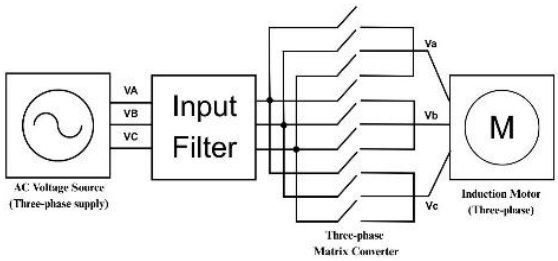

Figure 1. Block diagram of the three-phase matrix converter drive system

In induction motor drive applications, matrix converters offer an attractive alternative to rectifier–inverter based variable frequency drives. They can produce sinusoidal output currents and support full regenerative operation, making them suitable for high-efficiency and dynamic drive systems. The absence of a DC link also enhances reliability for critical industrial applications, particularly where power quality and power density are key requirements. [15]. The use of matrix converters in induction motor drives is supported by their capability to regulate both the output-voltage frequency and its magnitude, allowing precise adjustment of motor speed and torque. Modulation techniques such as Venturini modulation and Space Vector Modulation (SVM) are employed to produce smooth waveforms and achieve voltage transfer ratios of up to approximately 0.866 for conventional matrix converters [16].

2.2. Indirect Matrix Converter

Recent IMC topologies incorporate additional switching stages that enable AC–AC voltage boosting without the need for inductors or large capacitors. These developments allow the converter to achieve a unity voltage transfer ratio while maintaining system integrity and high-quality output waveforms. [11]. Recent decades have seen the development of various modulation strategies for controlling matrix converters, traditionally referred to as Direct Matrix Converter (DMC). In this context, the terms Matrix Converter and DMC are used interchangeably. More recently, the Indirect Matrix Converter (IMC) has gained prominence, offering the same input–output performance as the conventional converter while employing a simpler and more practical topology [17].

The IMC architecture comprises two principal conversion stages: an input-side converter and an output-side converter. The input stage functions as a three-phase–to– single-phase matrix rectifier formed using six bidirectional switching devices, and it operates in a current-source rectification mode that shapes the input currents toward sinusoidal profiles while generating a regulated average fictitious DC-link voltage. This intermediate voltage reflects the 'fictitious DC-link' principle introduced by Rodriguez and later refined by Holtz and Boelkens, who transformed the original DMC switching arrangement into the indirect topology that defines the IMC [17].

On the load-side stage, a traditional three-phase voltage-source inverter is adopted, comprising six unidirectional semiconductor switches responsible for shaping the output-voltage waveforms. Together, the two stages employ the same total number of active devices as a direct matrix converter, yet the IMC is considerably easier to implement because standard inverter modules can be used on the load side, and the number of active switches on the source side can be reduced to three when bidirectional power flow is not required [17].

The Indirect Matrix Converter (IMC) offers several compelling advantages over conventional conversion topologies (AC–DC–AC). Discarding the bulky DC-link capacitor enables the IMC to deliver a higher power density, reduced system size and weight, and improved reliability under high-temperature conditions. In addition, IMCs support sinusoidal input and output waveforms, bidirectional power flow, and controllable input power factor, making them highly suitable for dynamic motor-drive applications and critical industrial systems [18], [19].

2.3. Hysteresis-Based Direct Torque Control for Three-Phase Induction Motors

Hysteresis-based Direct Torque Control

(DTC) of a three-phase induction motor is a method in which the stator flux linkage and electromagnetic torque are estimated in the stationary α-β reference frame and then compared with their respective reference values using hysteresis comparators for both flux and torque. The resulting error signals are processed by a switching table that directly selects the inverter voltage vector to maintain the flux and torque within their predefined tolerance bands. This approach provides very fast dynamic response and eliminates the need for coordinate-transformation-based regulators or inner current-control loops [20].

In the context of a three-phase induction motor drive, this hysteresis-based DTC scheme exploits the direct link between stator voltage vector selection and motor electromagnetic behaviour: the stator flux vector is obtained by integrating the input voltages minus stator resistive drop, and torque is computed from the cross-product of estimated flux and stator currents. When either torque or flux leaves its hysteresis band, the controller chooses a new voltage vector from the inverter to bring them back—thereby achieving direct torque and flux regulation via hysteresis control [21].

3. RESEARCH METHODS

This paper demonstrates the proposed system through modelling and simulation in MATLAB/Simulink. The case study considers a variable-speed drive for an 11-kW, 400-V, 50- Hz three-phase induction motor supplied by an Indirect Matrix Converter (IMC) controlled using hysteresis-based Direct Torque Control (DTC). The reference speed can be adjusted according to the desired operating frequency, allowing the motor to operate over a wide range of speeds and load conditions.

3.1. Modeling of a Variable-Speed Drive Using an Indirect Matrix Converter

The grid source is modeled as a three-phase 400-V, 50-Hz equivalent feeding the Indirect Matrix Converter (IMC) through measurement interfaces. The IMC comprises two main stages. The line-side converter functions as a current- source rectifier using six bidirectional switches arranged in a three-phase–to–single-phase configuration. Its gating signals are provided by a 10-kHz PWM Generator operating in 3-arm bridge mode, with an internally generated modulating signal and adjustable modulation index to shape sinusoidal input currents and sustain the fictitious DC-link voltage.

The load-side converter is a three-phase voltage-source inverter built from six IGBTs with antiparallel diodes. Its switching states are determined by a hysteresis-based Direct Torque Control (DTC) algorithm, which selects voltage vectors to regulate the stator flux and electromagnetic torque of the induction motor. A braking chopper and resistor stabilize the virtual DC link during regenerative events. The full IMC–DTC drive is implemented in MATLAB/Simulink with a 5-µs time step to capture switching transients and motor dynamics.

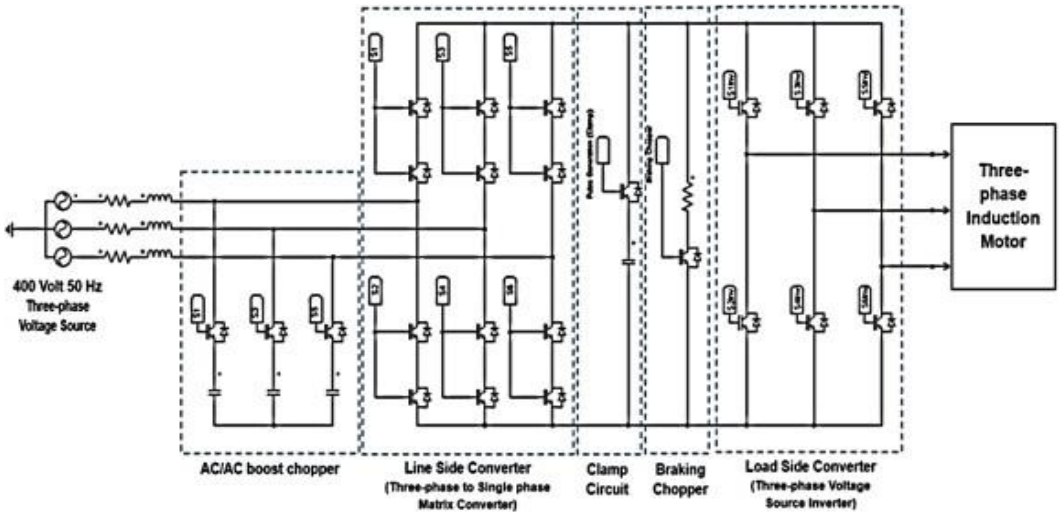

Figure 2. Overall topology of the proposed IMC-based AC–AC drive system, consisting of an AC/AC boost chopper, a three-phase–to– single-phase line-side matrix converter, a clamp circuit with braking chopper, and a three-phase voltage-source inverter supplying an induction motor.

Figure 2 illustrates the complete architecture of the IMC-based drive system, showing the AC/AC boost chopper, the line-side matrix converter, the clamp and braking circuits, and the load-side voltage-source inverter feeding the three-phase induction motor. The figure highlights the separation of gating strategies, where the PWM generator supplies the six pulses for the line-side converter, while the DTC controller determines the switching sequence of the load-side inverter.

3.2. Three-phase Induction Motor and Load Modeling

The load used in this study is an 11-kW, 400-V three-phase induction motor modeled using manufacturer equivalent motor parameters. The load torque is applied through the Load Torque block as a torque profile, allowing both no-load and loaded operating conditions to be simulated. The mechanical speed is measured in rad/s and converted to RPM for evaluating the drive's speed performance.

3.3. Architecture of the Direct Torque Control (DTC) Method

The hysteresis direct torque control scheme is structured around three major components:

3.3.1. Flux & Torque Calculation in Direct Torque Control (DTC)

The three-phase stator voltages (V_{abc}) and currents (I_{abc}) are transformed into the α-β reference frame using the Clarke transformation. The stator flux components ϕα- ϕβ are obtained through a first-order discrete integrator that accounts for the stator resistance. The flux magnitude and position are computed using the hypotenuse function (hypot) and the four-quadrant arctangent (atan2), respectively. The electromagnetic torque is then evaluated using the classical DTC expression based on the (id, iq) current components and the estimated stator flux.

Table 1. Technical Specifications of the Three-Phase Induction Motor

Parameter	Symbol	Value	Unit
Rated Power	Pn	11.000	W
Line Voltage (rms, L–L)	Vn	400	V
Frequency	fn	50	Hz
Pole Pairs	p	2	–
Stator Resistance	R_s	0.78	Ω
Rotor Resistance (referred)	Rr	0.40	Ω
Stator Leakage Inductance	Lls	2.5×10^{-3}	H
Rotor Leakage Inductance (referred)	Llr	2.5×10^{-3}	H
Magnetizing Inductance	Lm	0.14	H
Inertia	J	0.045	kg·m²
Viscous Friction	B	0.0035	N·m·s
Synchronous Speed	ωsyn	157	rad/s
Rated Torque	T_n	70	N·m
Nominal Stator Flux	ϕn	1.04	Wb

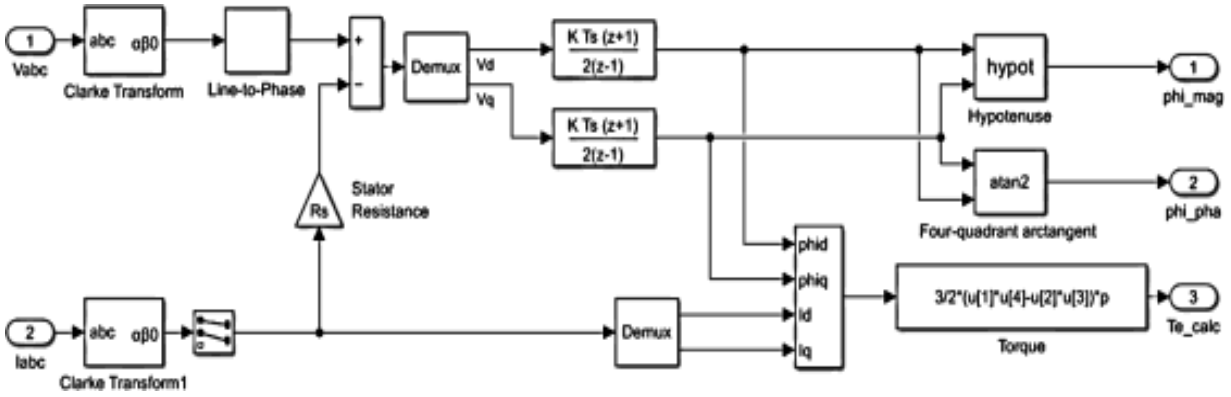

Figure 3. Structure of the flux and torque estimation stage in the Direct Torque Control scheme, including Clarke transformation, stator flux integration, flux magnitude and angle calculation, and electromagnetic torque computation

3.3.2. Hysteresis Control in Direct Torque Control (DTC)

The estimated torque and flux are compared with their reference values (T_e^* dan ϕ^*) using dedicated hysteresis bands. The outputs of the hysteresis comparators generate binary control signals that indicate whether the torque must be increased or decreased and whether the stator flux should be strengthened or weakened.

The hysteresis control block regulates the electromagnetic torque and stator flux by comparing their instantaneous values with the respective reference commands. The torque error $e_T=T_e^*-T_e$ processed using a two-level hysteresis comparator, which determines whether the torque needs to be increased or decreased based on its deviation from the allowable band. Similarly, the stator flux error $e_\phi=\phi^*-\phi$ is evaluated by a flux hysteresis controller that maintains the flux magnitude within a predefined tolerance range. These two comparator outputs form the primary switching decisions used by the DTC algorithm to select the appropriate voltage vector in real time. As a result, the inverter is switched according to the instantaneous flux angle and the torque–flux control requirements, achieving fast dynamic response without requiring current loops or PWM carriers.

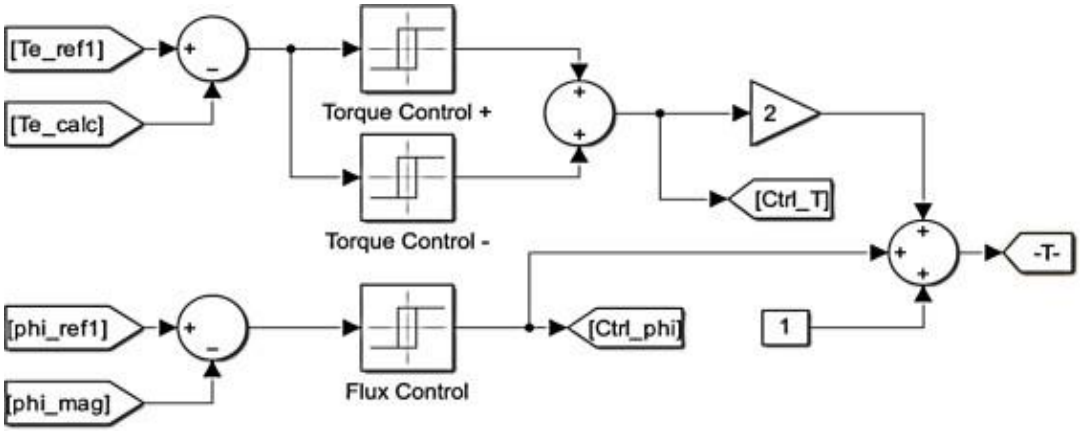

Figure 4. Hysteresis-based torque and flux control block used in the Direct Torque Control (DTC) scheme

In this work, both the torque and flux hysteresis bands are set to 8% of their nominal values, producing a symmetrical control window of ±4% around zero error. The torque hysteresis thresholds are defined as $\pm(0.08T_n/2)$, while the flux thresholds are given by $\pm(0.08\phi_n/2)$. When the torque error exceeds the upper boundary, the controller issues a command to increase torque; conversely, an error below the lower boundary triggers a torque reduction command. The same logic applies to the stator flux comparator.

This hysteresis configuration balances torque ripple and switching frequency, ensuring sufficiently smooth control action while maintaining the fast transient behavior characteristic of DTC. The combined torque–flux hysteresis decisions are then encoded into the control order, which directly guides the optimal switching block in selecting the corresponding voltage vector for the inverter.

3.3.3. VSI Switching Block within the Indirect Matrix Converter

The stator flux angle is used to determine the corresponding space-vector sector. The sector information, together with the torque hysteresis status, is supplied to the Determine Required Vector block, which is implemented as a two-dimensional lookup table. This block selects the optimal voltage vector index according to the conventional DTC switching table. The selected vector index is then passed to the Vector-to-Pulses block, which converts it into the switching pattern for the three-phase inverter. In the optimal switching stage, the flux angle estimated in the previous step is normalized into one of six space-vector sectors by the Determine Sector block. The resulting sector index is combined with the torque control signal generated by the hysteresis comparator and mapped through the two-dimensional lookup table to determine the required voltage vector.

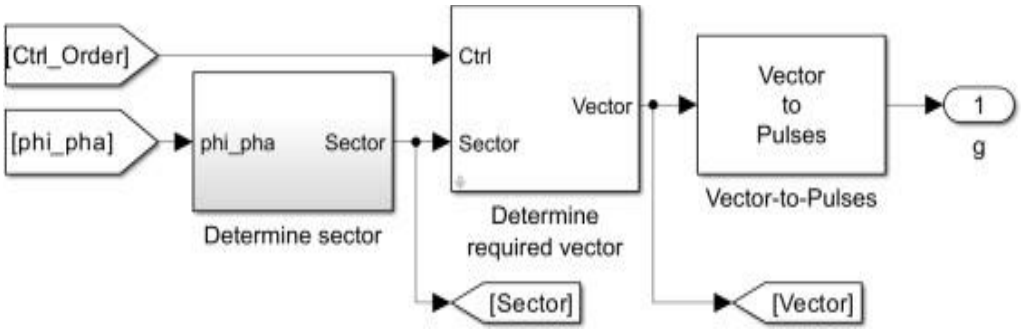

Figure 5. Sector identification, voltage-vector selection, and pulse generation block used in the Direct Torque Control (DTC) scheme

This mechanism ensures that the inverter applies the most suitable voltage vector to maintain the stator flux within the correct region while increasing or decreasing torque as commanded. The output of this block is translated into gate-level switching pulses for the inverter, enabling the fast dynamic response characteristic of Direct Torque Control. The resulting voltage-vector index is then passed to the Vector-to-Pulses block, which converts it into the corresponding gating signals for the three-phase inverter switches. This stage ensures that the applied voltage vector keeps the stator flux within the appropriate sector while increasing or decreasing the electromagnetic torque as required. Consequently, the algorithm produces an optimal switching pattern, which underpins the fast dynamic response characteristic of Direct Torque Control.

3.3.4. Design of the Speed Regulator

In Direct Torque Control (DTC), a speed control loop based on a PI regulator is employed to generate the torque reference. The speed reference ω_{ref} is obtained from the VSD input, where the desired operating frequency is converted into the corresponding synchronous speed in rad/s. This reference is compared with the actual motor speed ω_m, producing a speed error signal. The error is processed by a discrete PI regulator equipped with anti-windup and upper–lower torque limits. The anti-windup mechanism prevents integrator saturation when the torque command reaches its allowable limits, thereby maintaining controller stability during transient conditions and under heavy loading.

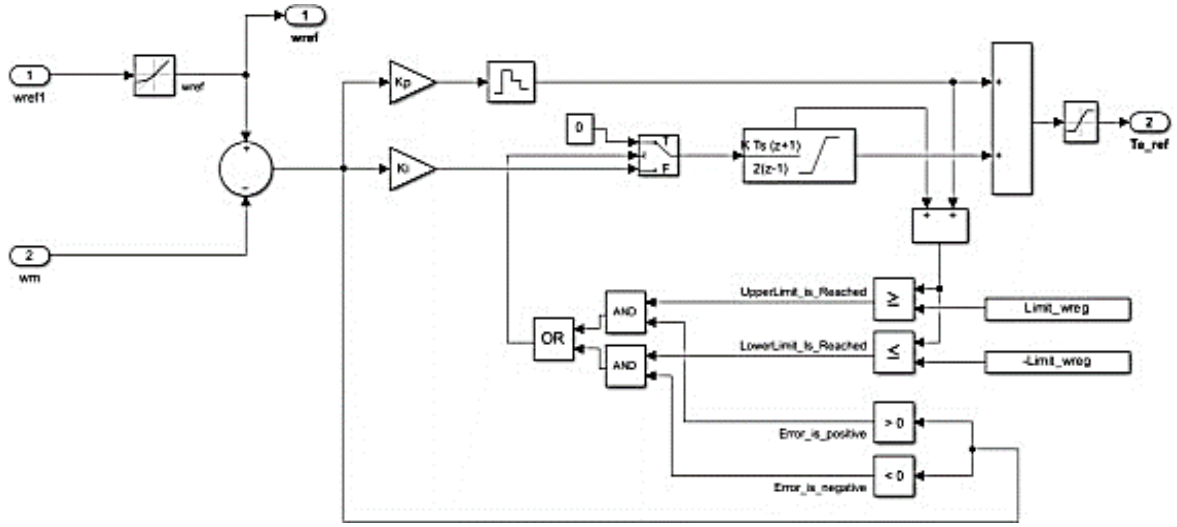

Figure 6. Discrete PI speed regulator with anti- windup and torque limiting used to generate the electromagnetic torque reference in the DTC drive

The PI controller supplies the torque reference T^*_e to the DTC block for hysteresis evaluation. With this configuration, speed regulation is achieved indirectly through torque control: the outer loop (speed) determines the required torque, while the inner loop (DTC) fulfills this request by selecting the appropriate voltage vector. This cascaded control structure is

widely used in DTC-based motor drives because it enables fast speed response, maintains torque within safe limits, and improves the robustness of the system against load disturbances.

3.4. Test Conditions and Measurement Parameters

The simulation study is conducted under two principal operating conditions:

- Gradual variations in the reference frequency or speed, encompassing start-up to nominal operation, and;
- Load-torque conditions, including both no- load operation and a constant mechanical load of 50 N·m.

For each case, the following electrical and mechanical quantities are captured using scope and RMS measurement tools:

- Grid-side voltages and currents (v_{grid}, i_{grid}).
- Fictitious DC-link voltage (v_{fdc}).
- stator voltages and currents (v_{abc}, i_{abc}).
- measured rotor speed in rpm (n_{meas}).

The recorded data are analyzed to evaluate the dynamic speed response, voltage regulation, and output characteristics of the unity-ratio Indirect Matrix Converter when supplying a DTC-based induction motor under varying operating conditions.

4. RESULTS AND DISCUSSION

4.1. Performance Evaluation Under No-Load Condition

Table 2 presents the no-load characteristics of the induction motor under several operating frequencies. The line-to-line output voltages increase proportionally with the applied frequency, indicating that the V/f ratio is preserved. The fictitious DC-link voltage V_{fdc} remains nearly constant at approximately 647–648 V for all test points, confirming stable unity–voltage-transfer operation of the IMC across the tested range.

Table 2. No-Load Test of the Induction Motor

f (Hz)	V_{ab} (V)	V_{ac} (V)	V_{bc} (V)	V_{fdc} (V)	$I_{s(rms)}$ (A)	n_{sync} (rpm)	n_{meas} (rpm)	t_{ss} (s)	Slip (%)
10	203.4	203.4	203.4	648.03	5.73	300	300	0.503	0.00%
25	320.8	320.9	320.9	647.94	5.73	750	750	1.251	0.00%
50	453.7	454.0	454.1	647.65	5.75	1500	1500	2.501	0.00%
60	497.3	497.1	497.1	647.56	5.75	1800	1800	3.005	0.00%

Table 3. Measured Characteristics of the Induction Motor Under 50 N.m Step-Load Torque at t = 3s

f (Hz)	V_{ab} (V)	V_{ac} (V)	V_{bc} (V)	V_{fdc} (V)	$I_{s(rms)}$ (A)	n_{sync} (rpm)	n_{meas} (rpm)	t_{ss} (s)	$t_{ss\text{-}step}$ (s)	Slip (%)
10	246.5	234.5	242.6	637.64	14.7	300	300	0.503	0.485	0.00%
25	338.2	327	338.4	625.89	14.5	750	750	1.251	0.541	0.00%
50	452.7	456.3	450.1	605.17	14.6	1500	1500	2.501	0.429	0.00%
60	484.2	488.9	488.9	596.90	14.7	1800	1782.4	3	-	0.98%

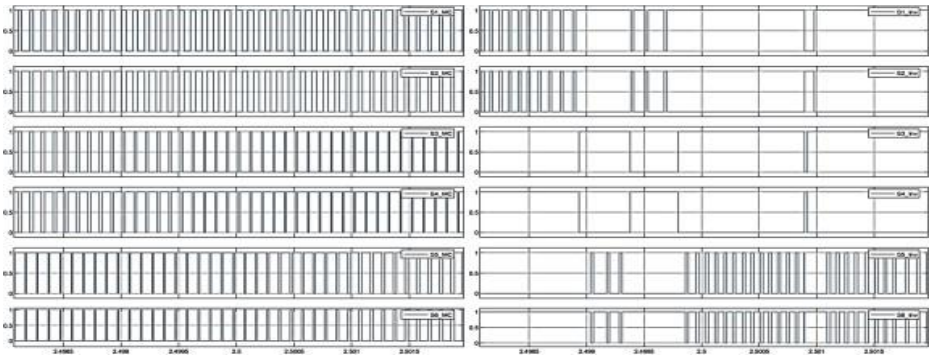

Figure 7. Sample of gating signals captured from 2.4985 s to 2.5015 s. The left traces (S1 MC–S6 MC) show the carrier-based PWM pulses driving the line-side matrix converter, while the right traces (S1 Inv–S6 Inv) display the hysteresis-based DTC switching commands for the load-side inverter.

The stator current I_s^{rms}, defined as the averaged RMS current of the three stator phases, remains within 5.73–5.75 A for all frequencies. This aligns with the expected behavior of an induction motor under no-load conditions, where the magnetizing current dominates and remains relatively insensitive to frequency variations when V/f is maintained. The measured speed n_{meas} matches the synchronous speed n_{sync} at each operating frequency, resulting in a slip of 0.00%, which is typical for no-load operation in an ideal simulation environment with negligible mechanical losses. The settling time t_{ss} defined as the time required for the motor to reach steady-state speed from standstill, increases with the target operating frequency. At 10 Hz the motor reaches steady-state in approximately 0.503 s, whereas at 60 Hz it requires about 3.005 s. This increase reflects the longer acceleration interval required to achieve higher final speeds.

Overall, the results demonstrate that the IMC-driven DTC system maintains stable voltage, minimal slip, and predictable speed response under no-load conditions. The Figure 8 illustrates the dynamic response of an induction motor drive based on an Indirect Matrix Converter (IMC) controlled by Direct Torque Control (DTC) under no-load operation at a 10-Hz reference frequency. Several subplots are presented, showing the input voltage and current, the fictitious DC-link voltage, the filtered stator voltage and current, and Figure 9 illustrates the rotor speed over a 0–5 s simulation window. At the Figure 8, the three-phase grid voltage (v_{grid}) appears balanced and sinusoidal, followed by low-amplitude grid currents (i_{grid}) that reflect the light loading of the IMC under no-load conditions. The fictitious DC-link voltage (v_{fdc}) exhibits a stable switching pattern with a constant average level, confirming proper energy conversion on the converter input side.

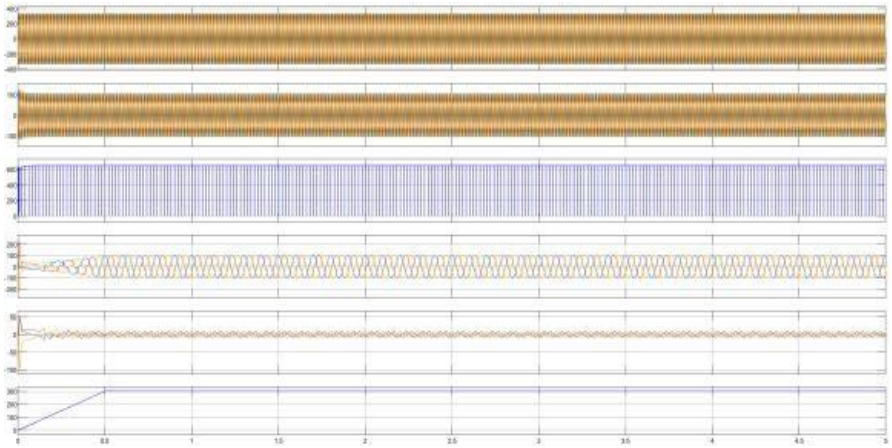

Figure 8. Waveforms of the IMC–DTC induction motor drive under no-load operation at 10 Hz, showing grid-side voltages/currents, fictitious DC-link voltage, filtered stator voltages/currents, and rotor speed reaching 300 rpm.

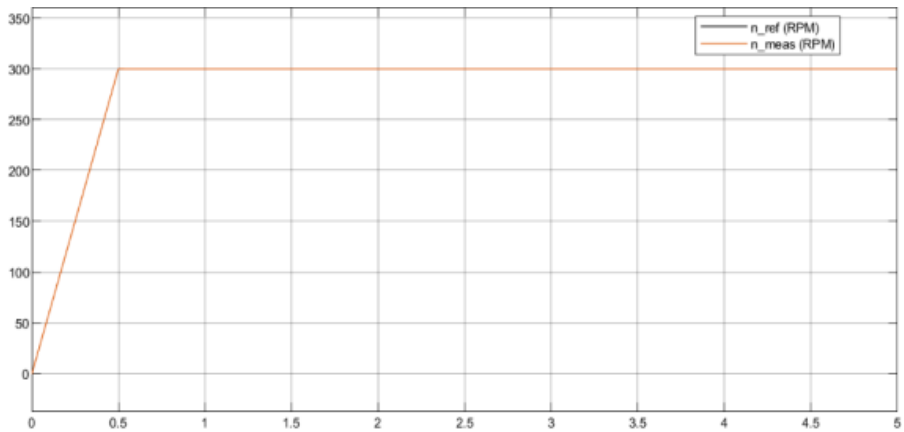

Figure 9. Speed reference and measured rotor speed of the IMC–DTC induction motor drive during no-load operation at 10 Hz

The rotor settles at approximately 300 rpm, resulting in a slip of 0.00%. The subsequent subplots display the low- pass-filtered stator voltage (v_{abc}), which shows an initially transient waveform before settling into a steady sinusoidal shape. The stator currents (i_{abc}) remain very small (approximately 5–6 A), consistent with an unloaded induction machine. At the Figure 9, the rotor speed n(t) rises linearly during the initial acceleration phase and reaches the synchronous value of about 300 rpm at t ≈ 0.5 s, after which it remains steady. This indicates that the speed loop and DTC algorithm regulate the machine effectively in the absence of load torque. Overall, the figure demonstrates a stable low-frequency response of the IMC–DTC drive, characterized by balanced waveforms, low stator current, and smooth acceleration during no-load operation.

4.2. Evaluation of Motor Performance Under Step-Load Torque

The subsequent test assesses the induction motor's performance under a steady load torque of 50 N·m, followed by an additional step load introduced at t = 3s. The results of this test are summarized in Table 3 on the preceding page. The line-to-line output voltages (V_{ab}, V_{ac}, V_{bc}) increase with operating frequency, while the fictitious DC-link voltage V_{fdc} remains within a narrow range (596–638 V), indicating that the Indirect Matrix Converter maintains a consistent voltage-transfer ratio under loaded conditions.

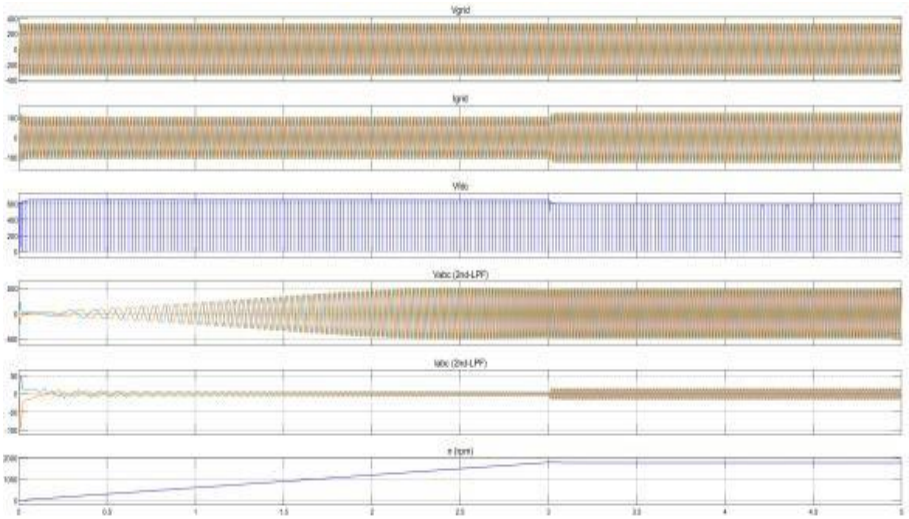

Figure 10. Waveform responses of the IMC– DTC induction motor drive at 60 Hz under a 50 N·m load. The plots show grid voltage, grid current, fictitious DC-link voltage, filtered stator voltages and currents

The stator RMS current I^{rms} remains approximately 14.5–14.7 A for all$_s$ operating frequencies. This is expected because the electromagnetic torque required to counter the 50 N.m load is primarily determined by the q-axis component of the stator current, which remains relatively constant regardless of operating frequency. The measured motor speed n_{meas} matches the synchronous speed for 10, 25, and 50 Hz, resulting in zero slip under simulated no-loss conditions. At 60 Hz, the measured speed is 1782.4 rpm, corresponding to a slip of approximately 0.98%, which is consistent with the increased load at higher speed. The settling time from standstill, t_{ss} increases proportionally with the target operating speed, ranging from 0.503 s at 10 Hz to 3.0 s at 60 Hz. The additional parameter $t_{ss\text{-}step}$ captures the transient response following the torque step at $t = 3$ s. The motor demonstrates rapid recovery across all frequencies, with settling times between 0.429 and 0.541 s, except for 60 Hz where the system is already in steady-state immediately prior to the step application.

Overall, the results confirm that the IMC–DTC system maintains stable current, acceptable slip, and predictable transient behavior under load torque disturbances. Figure 10 illustrates the response of the induction motor drive employing the IMC– DTC scheme when operated at 60 Hz under a steady-state load torque of 50 N·m. The grid voltage and current ($V_{\text{grid}}, I_{\text{grid}}$)exhibit clean

sinusoidal profiles, indicating proper operation of the input-side converter and a well-maintained power factor. The fictitious DC-link voltage (V_{fdc}) remains nearly constant, with minor ripple attributed to the switching action of the IMC. The low-pass-filtered stator voltage (V_{abc}) and stator current (I_{abc}) show balanced three-phase waveforms following the initial transient. The stator current amplitude is noticeably higher than in the no-load condition, which is consistent with the torque demand of 50 N·m at 60 Hz.

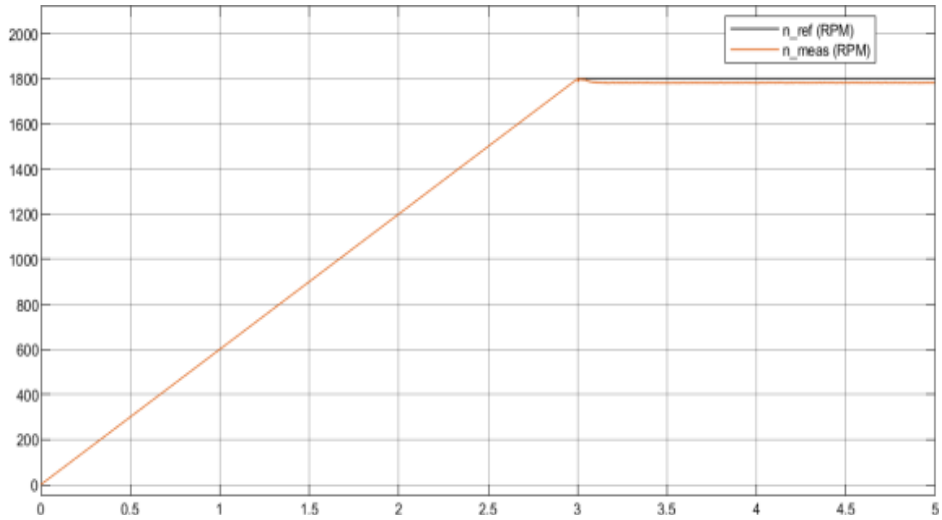

Figure 11. Rotor-speed response of the IMC– DTC induction motor drive under 60 Hz and 50 N·m load: the measured speed converges to ~1782 rpm (≈0.98 % slip relative to the 1800 rpm reference)

Figure 11 shows sinusoidal waveforms with the rotor speed converging to about 1782 rpm, corresponding to a slip of nearly 0.98%, which is characteristic of an induction machine under moderate load. The steady-state speed is reached at about t ≈ 3 s, and the system remains stable thereafter. Overall, the results confirm that the unity-ratio IMC with DTC control maintains balanced stator voltages, regulates current according to the torque requirement, and delivers stable speed regulation even under a 50 N·m torque load.

5. CONCLUSION

This study evaluated the performance of an Indirect Matrix Converter (IMC) with a unity voltage transfer ratio for driving a three-phase induction motor under a hysteresis-based Direct Torque Control (DTC) scheme. The MATLAB/Simulink model developed in this work shows that the IMC is able to maintain a stable fictitious DC-link voltage over a wide range of operating frequencies produce balanced output voltages, and ensure sinusoidal input currents with a controllable power factor.

Under no-load conditions, the motor reached its synchronous speed with zero slip and exhibited a consistent magnetizing current. When subjected to a 50 N·m torque load, the system demonstrated behavior consistent with induction motor theory, including slip values between0-0.98 percent and smooth acceleration.

The transient response to torque disturbances showed recovery times of approximately 0.43 to 0.54 seconds at most operating points, indicating good dynamic characteristics and stable torque–flux regulation. Overall, the results confirm that a unity-ratio IMC is suitable for variable-speed drive applications and provides a compact, efficient, and reliable alternative to conventional AC–DC–AC converters with DC- link capacitors. For further development, future work is recommended to evaluate IMC performance under dynamic, nonlinear, and regenerative load conditions to assess the robustness of the clamp circuit and braking chopper. Additional improvements may include the implementation of more advanced control strategies such as Space Vector Modulated matrix converter control, predictive control, or adaptive hysteresis techniques to reduce torque ripple and improve switching efficiency.

REFERENCES

[1] M. Azab, "A Review of Recent Trends in High-Efficiency Induction Motor Drives," Vehicles, vol. 7, no. 1, p. 15, Feb. 2025, doi: 10.3390/vehicles7010015.

[2] P. Dinolova, V. Ruseva, and O. Dinolov, "Energy Efficiency of Induction Motor Drives: State of the Art, Analysis and Recommendations," Energies (Basel), vol. 16, no. 20, p. 7136, Oct. 2023, doi: 10.3390/en16207136.

[3] U. Sengamalai, G. Anbazhagan, T. M. Thamizh Thentral, P. Vishnuram, T. Khurshaid, and S. Kamel, "Three Phase Induction Motor Drive: A Systematic Review on Dynamic Modeling, Parameter Estimation, and Control Schemes," Energies (Basel), vol. 15, no. 21, p. 8260, Nov. 2022, doi: 10.3390/en15218260.

[4] I. K. Wiryajati and I. N. W. Satiawan, "Open-Loop Performance Analysis of Induction Motors under V/f Speed Control," Dielektrika –Jurnal Ilmiah Kajian Teori dan Aplikasi Teknik Elektro, vol. 12, no. 2, pp. 22–31, Aug. 202AD.

[5] A. Abdel-Aziz, M. A. Elgenedy, and B. Williams, "A Comparative Review of Three Different Power Inverters for DC– AC Applications," Energies (Basel), vol. 16, no. 21, p. 7254, Oct. 2023, doi: 10.3390/en16217254.

[6] G. Mazzanti, B. Diban, E. Chiodo, P. De Falco, and L. P. Di Noia, "Forecasting the Reliability of Components Subjected to Harmonics Generated by Power Electronic Converters," Electronics (Basel), vol. 9, no. 8, p. 1266, Aug. 2020, doi: 10.3390/electronics9081266.

[7] Hironimus, Linda Sartika, and Abdul Muis Prasetia, "Power Analysis of 3 Phase Induction Motor Drive Conveyor 06 at PT. Mitrabara Adiperdana," Electrician : Jurnal Rekayasa dan Teknologi Elektro, vol. 18, no. 2, pp. 153–160, May 2024, doi: 10.23960/elc.v18n2.2587.

[8] Gamar Basuki, Era Purwanto, Hary Oktavianto, Mentari Putri Jati, and Mochamad Ari Bagus Nugroho, "Aplikasi Direct Matrix Converter pada Pengendali Kecepatan Motor Induksi 3 Fase menggunakan Modulasi Venturini," ELKOMIKA, vol. 8, no. 3, pp. 518–532, Sep. 2020.

[9] Mentari Putri Jati, Era Purwanto, Bambang Sumantri, and Gamar Basuki, "Matrix Converter sebagai Pengendali Kecepatan Motor Induksi 3 Fase dengan ISVM," ELKOMIKA, vol. 8, no. 2, pp. 373–387,May 2020.

[10] Muh. Novian Hadi Zaen, I Ketut Wiryajati, and I Made Ari Nrartha, "Pengaturan Kecepatan Motor Induksi 3 Phasa Menggunakan Matrix Konverter dengan Metode Sliding Mode Control," Dielektrika – Department of Electrical Engineering University of Mataram, vol. 10, no. 2, pp. 179–188, Aug. 2023.

[11] A. Jahangiri and A. Radan, "Indirect matrix converter with unity voltage transfer ratio for AC to AC power conversion," Electric Power Systems Research, vol. 96, pp. 157–169, Mar. 2013, doi: 10.1016/j.epsr.2012.11.008.

[12] Q.-H. Tran, H.-C. Vu, and H.-N. Nguyen, "Multimode space-vector overmodulation technique for enhancing voltage transfer ratio in matrix converters," Journal of Measurement, Control, and Automation, vol. 29, no. 1, pp. 26–32, Mar. 2025, doi: 10.64032/mca.v29i1.253.

[13] N. Dinh Tuyen and L. Minh Phuong, "SVPWM Method for Multilevel Indirect Matrix Converter with Eliminate Common Mode Voltage," Applied Sciences, vol. 9, no. 7, p. 1342, Mar. 2019, doi: 10.3390/app9071342.

[14] H. Wang, Y. Zhang, M. Su, Y. Sun, X. Li, and G. Zhang, "Control method for the two-stage matrix converter to enhance the linear voltage transfer ratio," IET Power Electronics, vol. 11, no. 14, pp. 22952301, Nov. 2018, doi: 10.1049/iet-pel. 2018.5388.

[15] A. von Jouanne, E. Agamloh, and A. Yokochi, "A Review of Matrix Converters in Motor Drive Applications," Energies (Basel), vol. 18, no. 1, pp. 1–28, Jan. 2025, doi: 10.3390/en18010164.

[16] M. Ali, A. Iqbal, and M. Khalid, "A Review on Recent Advances in Matrix Converter Technology: Topologies, Control, Applications, and Future Prospects," Int J Energy Res, vol. 2023, pp.1–28, Aug. 2023, doi: 10.1155/2023/ 6619262.

[17] D. Varajão and R. E. Araújo, "Modulation Methods for Direct and Indirect Matrix Converters: A Review," Electronics (Basel), vol. 10, no. 7, p. 812, Mar. 2021, doi: 10.3390/electronics10070812.

[18] A. von Jouanne, E. Agamloh, and A. Yokochi, "A Review of Matrix Converters in Motor Drive Applications," Energies (Basel), vol. 18, no. 1, p. 164, Jan. 2025, doi: 10.3390/en18010164.

[19] M. Ali, A. Iqbal, and M. Khalid, "A Review on Recent Advances in Matrix Converter Technology: Topologies, Control, Applications, and Future Prospects," Int J Energy Res, vol. 2023, pp. 1–28, Aug. 2023, doi: 10.1155/2023/6619262.

[20] A. A. Kadum, "New adaptive hysteresis band width control for direct torque control of induction machine drives," International Journal of Power Electronics and Drive Systems (IJPEDS), vol. 11, no. 4, p. 1908, Dec. 2020, doi: 10.11591/ijpeds.v11. i4.pp1908-1917.

[21] S. Lakhimsetty, V. S. P. Satelli, R. S. Rathore, and V. T. Somasekhar, "Multilevel Torque Hysteresis-Band Based Direct-Torque Control

Strategy for a Three-Level Open-End Winding Induction Motor Drive for Electric Vehicle Applications," IEEE J Emerg Sel Top Power Electron, vol. 7, no. 3, pp. 1969–1981, Sep. 2019, doi: 10.1109/JESTPE.2018.2870382.